MECHANICAL CHARACTERIZATION OF MATRIX-INDUCED AUTOLOGOUS CHONDROCYTE IMPLANTATION (MACI) GRAFTS FOR ARTICULAR CARTILAGE REPAIR

A Thesis

Presented to the Faculty of the Graduate School

of Cornell University

In Partial Fulfillment of the Requirements for the Degree of

Master of Science in Mechanical Engineering

by

Devin James Lachowsky

August 2012

ABSTRACT

Matrix-induced autologous chondrocyte implantation (MACI ®) is a cartilage repair technique that uses cells seeded in a type I/type III collagen membrane to assist in tissue formation within a defect site. There is minimal research on the long-term mechanical performance of these grafts in a large animal model. Two defects (15 mm) were placed in the lateral trochlear ridge of the right or left joint of 27 horses (1.5-6 years, 300-400 kg). The defects were filled with the following treatment options: 1) MACI and membrane alone (n=12); 2) empty and MACI (n=12); 3) 2 empty (n=3). The contralateral joint was left untouched for control. At 1 year post-implantation, two 3 mm plugs were removed from the defect and control tissue to be used for confined compression testing (to determine aggregate modulus and hydraulic permeability) and confocal strain mapping (to determine global and local shear modulus). In compression, MACI grafts had modulus and permeability values that were not statistically different than control and performed better than the other repair groups ($p<0.05$). In shear, all repair groups were significantly lower than the control shear modulus and showed little variation with depth from the articular surface. Mechanical testing suggests that MACI grafts are able to retain native compressive properties but not native shear properties. This study further characterizes the mechanisms of cartilage repair and performance of MACI grafts.

BIOGRAPHICAL SKETCH

Devin James Lachowsky, 27, is a native of Saint Paul, MN, the third of four children of a social worker and a registered nurse. He graduated from the University of Wisconsin, Madison in 2008 with a Bachelor's Degree in Mechanical Engineering. He lived for two years in New York City before deciding to pursue a graduate degree in Mechanical Engineering at Cornell University, graduating in 2012. His primary professional pursuit is to apply his engineering skills to the advancement of medical knowledge. In his spare time, he enjoys playing hockey and maintaining his vintage Volkswagen.

ACKNOWLEDGEMENTS

- Committee Members
    - Dr. Lawrence Bonassar (Advisor)
    - Dr. Jonathon Butcher
- Bonassar Lab
    - Darvin Griffin
    - Eddie Bonnevie
    - Dr. Natalie Galley
- Itai Cohen Group
    - Jesse Silverberg
- Cornell Vet School
    - Dr. Alan Nixon
- Genzyme Corporation
    - Study No. GENZ09-4417

TABLE OF CONTENTS

A. INTRODUCTION

1. Structure of Articular Cartilage

Articular cartilage is a connective tissue that coats the ends of bones in synovial joints. The tissue transfers the load of the body between bones while still allowing the joint to articulate. The surface of articular cartilage has a low coefficient of friction, creating a smooth surface that helps prevent wear.

The tissue structure can be broken down to approximately 30% extracellular matrix (ECM) and 70% water [2]. The only cells contained in cartilage are chondrocytes, which build and maintain the matrix. The ECM is composed of a series of proteoglycan monomers that bind to hyaluronic acid to form proteoglycan aggregates (Figure 1). The monomers contain two types of glycosaminoglycans (GAGs), keratin and chondroitin sulfate, both of which are extremely hydrophilic. Because of this, water is attracted to the GAGs and retained within the cartilage structure.

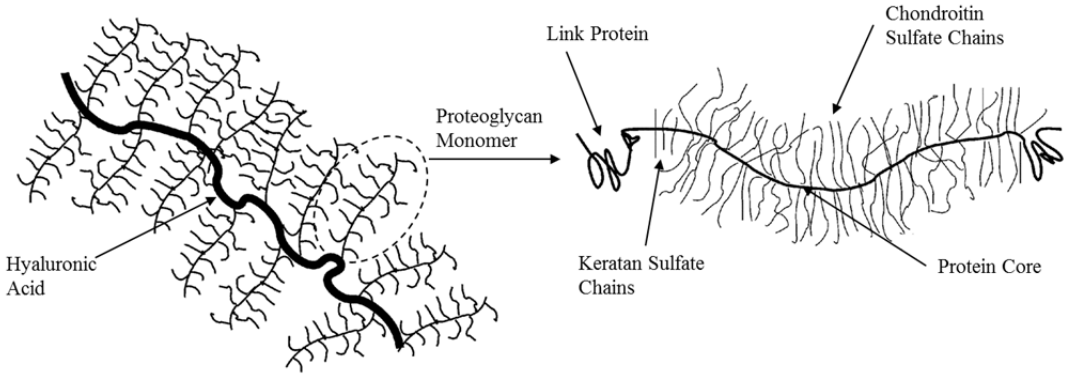

Figure 1: The structure of proteoglycans. Several proteoglycan monomers bind to hyaluronic acid through a link protein to form aggregates. GAG chains radiate from a protein core and retain water within the cartilage structure. (Reprinted with permission [1].)

The ECM also contains type II collagen fibers that have varying orientation with respect to position in cartilage (Figure 2). In the superficial tangential zone, the fibers tend to be parallel

with the surface, and in the deep zone, fibers tend to be perpendicular to the surface. The fibers are more randomly oriented in the middle zone. Cartilage calcifies deep into the tissue (indicated by the tidemark).

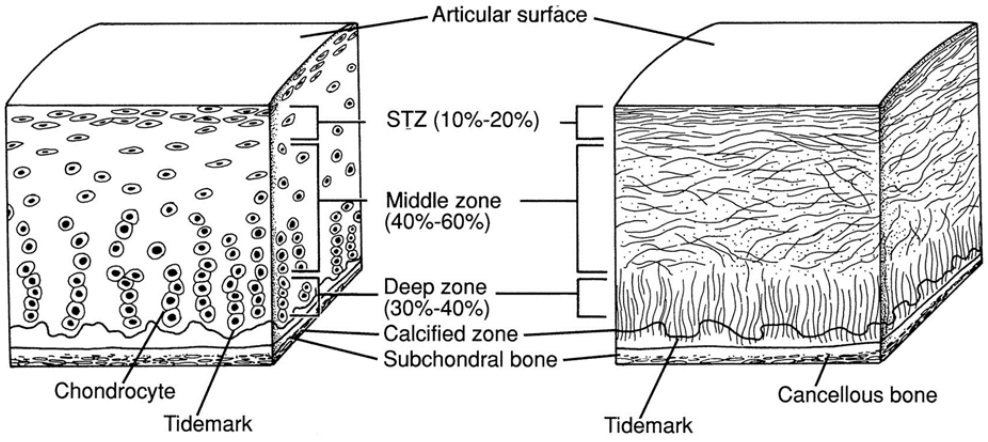

Figure 2: The arrangement of chondrocytes and collagen fibers within articular cartilage. (Reprinted with permission [3]).

The many structural complexities in articular cartilage are responsible for the anisotropy and inhomogeneity observed in the tissue's mechanical properties. Cartilage is viscoelastic because the magnitude of stress and strain in the material is time dependent. It is also poroelastic, because the tissue's rate of deformation is dependent on its permeability. Though there are several mechanical properties to consider when characterizing cartilage, much of its performance can be described by its compressive and shear properties.

a. Compression:

The compressive properties of cartilage are heavily influenced by its hydraulic permeability k. Specifically, the stiffness of cartilage is dependent on the flow rate of water in the tissue during compression. The flow rate Q can be described by Darcy's law, where dP/dx is the pressure gradient in the tissue:

$$Q = k\frac{dP}{dx} \quad (1)$$

Deformation of cartilage increases the pressure gradient, and therefore increases the flow of liquid from the tissue. However, as deformation increases, pore sizes in the tissue decrease and the permeability reduces. So while the deformation of cartilage is a function of permeability, its permeability is also a function of deformation.

As water flows from the cartilage, the pressure gradient decreases, and the stress within the cartilage relaxes. The relationship between the equilibrium stress and strain is described by the aggregate modulus Ha. Typical values for the aggregate modulus and permeability in human articular cartilage are 0.70 MPa and 1.18×10^{-15} m^4/N-s, respectively [(4)].

b. Shear:

The shear properties of cartilage vary heavily with depth from the articular surface. In general, the shear modulus is significantly lower near the surface and significantly higher in the deep zone. The purpose of the compliant region near the surface is not known, though some hypotheses suggest that it helps with energy dissipation and lubrication, thereby improving the durability of the articular surface [(5)].

2. Injury & Disease

Damage to articular cartilage can be caused by both traumatic injuries and disease. Repair to damaged cartilage is a very slow process. The tissue does not contain any blood vessels, so development of a new ECM is limited. Furthermore, chondrocytes are unable to migrate to

damaged tissue. When healing does occur, the repair tissue is often fibrocartilage rather than hyaline cartilage caused by the blood supply of the subchondral bone.

Osteoarthritis (OA) is a degenerative joint disorder marked by degradation of articular cartilage in a joint. Potentially, this can allow the subchondral bones in the joint to come in contact with each other, causing pain and swelling. Although the exact cause of OA is unknown, it has been observed that the proteoglycan content of cartilage reduces with age [(6)]. As a result, the water content decreases, making the tissue less robust and more susceptible to damage.

Traumatic injuries can result in immediate pain and swelling. If an injury is left untreated, it can often cause further wear to the joint. In addition, untreated injuries greatly increase the likelihood that OA will progress in the joint [(7)].

3. Treatment

There is no cure for OA, only treatment that can help relieve pain and increase mobility. There are, however, several treatment options to help repair damaged cartilage due to injury, and these treatments can help prevent the onset of OA. Some of these methods include debridement, microfracturing, and osteochondral autografts and allografts. While all of these methods have been shown to reduce pain in patients, none of them have been shown to recreate hyaline-like cartilage in the defect. One promising method for cartilage repair is a process known as autologous chondrocyte implantation (ACI).

Genzyme's Carticel ® is the only FDA approved ACI treatment in the United States. Treatment using ACI involves filling a defect with chondrocytes that are cultured using the patient's own cartilage. The defect is cleaned using a debriding tool. A small patch of periosteum is removed from the shin bone of the patient, and sutured over the defect to neighboring

cartilage. The cultured chondrocytes are then injected under the periosteal flap [8]. Despite the improvements in repaired tissue using this method, there are several shortcomings due to the periosteal flap. Using the flap increases the risk of graft hypertrophy, the sutures can damage the neighboring tissue, and the flap can delaminate and allow cells to leak into the joint [9] [10] [11]. An improvement on ACI is a procedure called matrix-induced autologous chondrocyte implantation (MACI ®, Genzyme Corporation). The procedure is very similar to ACI, except the chondrocytes are seeded in a porcine-derived type I/type III collagen bilayer membrane (see Figure 3 for full procedure) [9] [12]. On top of eliminating the shortcomings above, MACI grafts require fewer surgical procedures because the periosteum is no longer harvested. In addition, the collagen membrane helps maintain chondrocyte viability and phenotype, and potentially allows for a more even distribution of cells in the defect [13] [14].

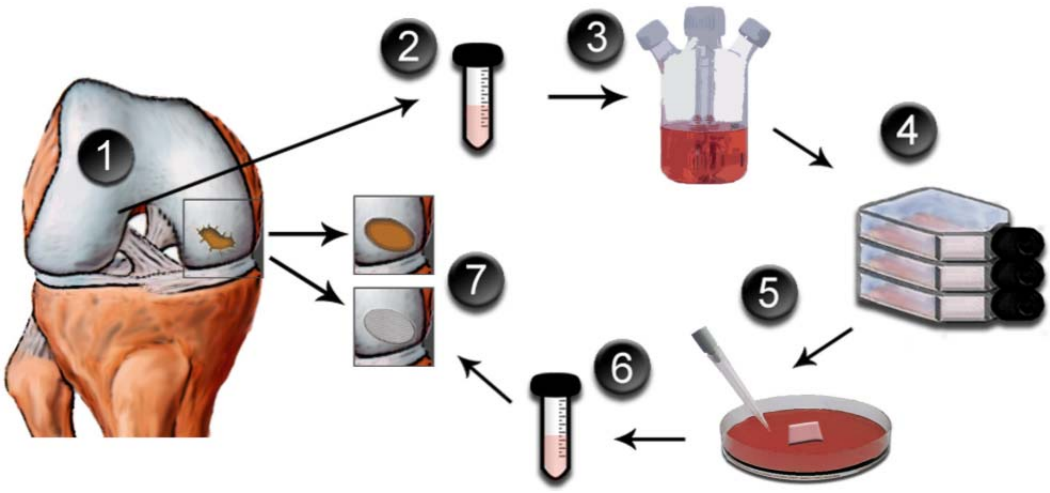

Figure 3: Steps to prepare and install MACI grafts: 1) A biopsy is taken of healthy articular cartilage; 2) the cartilage is sent to cell culture facility; 3) and enzymatically digested; 4) the chondrocytes are cultivated for several weeks; 5) the cells are seeded into the collagen membrane; 6) the implant is returned to the surgeon; 7) the injured cartilage is debrided, and the membrane is cut to size, installed into the defect, and secured with fibrin glue. (Reprinted with permission [11].)

Similar to the ACI implants, defects filled with MACI grafts have been shown to produce hyaline-like cartilage [8] [15]. There are several hundred journal articles that investigate the use of autologous chondrocytes, and nearly fifty that specifically look at MACI grafts (Pubmed).

However, the vast majority of these articles focus on the performance of the grafts through histologic examinations, biochemical analyses, and range of motion and pain evaluations. Only a handful of papers could be found that consider the mechanical performance of autologous chondrocyte grafts, and a summary of these studies is shown in Table 1.

The testing parameters from each study varied greatly, and as a result, the mechanical performance of each implant (normalized to the mechanical performance of native articular cartilage) also varied significantly. The duration of implanted tissue ranged from as short as a few weeks to as long as several years. The defect size ranged from 3 mm to 15 mm in animal models as small as mice and rabbits and as large as horses and humans. A general trend shown in this data is that samples in larger animals and with longer implant durations tend to perform better, indicating that mechanical properties of repaired cartilage may improve over time. The defect size and choice of animal model likely impact mechanical performance as well, though a general trend is not as apparent.

None of the studies in Table 1 perform an exhaustive list of mechanical tests on autologous chondrocyte grafts. Compressive properties were mostly found through indentation tests that estimate a Poisson's ratio and assume material homogeneity. In addition, there are no known papers that look at the shear properties of the repaired cartilage, which has been shown to locally change in native tissue [(5)]. The research done to this point is not sufficient to predict the full mechanical behavior of MACI grafts in a long-term, large animal model. It is necessary to perform a full array of mechanical tests in order to fully understand this behavior. Established methods for determining the compressive and shear properties of articular cartilage are confined compression testing and confocal strain mapping, respectively [(5)] [(16)].

Table 1: Experiments that have analyzed the mechanical properties of autologous chondrocyte-based cartilage repairs. The treatment method of each experiment is listed along with the membrane material (if applicable).

Treatment Method	Duration	Animal Model	Defect Size	Mechanical Test	Properties Measured	Performance (normalized to native tissue)
Allogenic Chondrocytes [17]	8 mos.	Equine	15 mm	Tension	Tensile Modulus	48%
ACI [18]	8 mos.	Equine	15 mm	Confined Compression	Dynamic Modulus Aggregate Modulus	50% 12%
ACI [19]	6 mos.	Porcine	7 mm	Unconfined Compression	Aggregate Modulus	39%
ACI [20]	3 mos.	Porcine	6 mm	Indentation	Stiffness	32%
ACI [21]	33-84 mos. (mean 54.3 mos.)	Human	varied	Indentation	Stiffness	75%
ACI [22]	4-51 mos. (mean 22.1 mos.)	Human	varied	Indentation	Stiffness	100%
MACI [23] 1) Type I/Type III collagen 2) Type II collagen	12 mos.	Ovine	7 mm	Indentation	Stiffness	 50% 37%
MACI [24] Type I/Type III collagen	8,10,12 wks.	Ovine	6 mm	Partially confined compression	Stiffness	16%
MACI [25] [26] Type II collagen	15 wks.	Canine	4 mm	Indentation	Dynamic Modulus Aggregate Modulus	5% 15%
MACI [27] Type I collagen, hyaluronan, fibrin	6 wks.	Leporine	3 mm	Unconfined Compression	Stiffness	20-70%*
MACI [28] Catilage chips, fibrin	9 wks.	Mouse	6 mm	Confined Compression	Aggregate Modulus	90 kPa**
MACI [29] PGA, Pluronic	24 wks.	Porcine	8 mm	Compression	Stiffness	60%

* See paper.
** No comparison to native cartilage available.

a. Background on Genzyme Project

Genzyme has prepared study number GENZ09-4417 in order to test the efficacy of MACI grafts in an equine model. A total of 27 skeletally mature horses (mixed breeds, ages 1.5-6 years, weights 300-400 kg) were approved according to the guidelines of the Institutional Animal Care and Use Committee (IACUC) at Cornell University. The horses were given initial and routine screenings for orthopaedic abnormalities in their hind limbs.

Table 2: Listing of the treatment pairs used to fill the two defects in each operated joint.

Repair Group Pair	Treatment	Group	Number of Horses
1	MACI graft ACI-Maix membrane (alone)	A B	12
2	Empty defect MACI graft	C D	12
3	Empty defect Empty defect	E	3

Each horse contained one operated joint with two full thickness defects placed 25 mm apart in the lateral trochlear ridge (Figure 4). The defects were made using a 15 mm coring tool, with any remaining cartilage debrided with a periosteal elevator. The defects were filled with the following three treatment options: 1) MACI grafts with ACI-Maix membrane; 2) ACI-Maix membrane alone; 3) Defects left empty. MACI grafts were implanted in defects using Genzyme's standard operating protocol. A biopsy was made in the femoro-patellar joint using a periosteal elevator. Cartilage was removed from the joint, and chondrocytes were isolated, expanded in culture, and finally seeded in the ACI-Maix membrane. The membrane was then cut to size and adhered to the subchondral bone using fibrin glue (Figure 3). ACI-Maix membranes

alone were installed in the same fashion as MACI grafts, but with no chondrocytes seeded in the membrane.

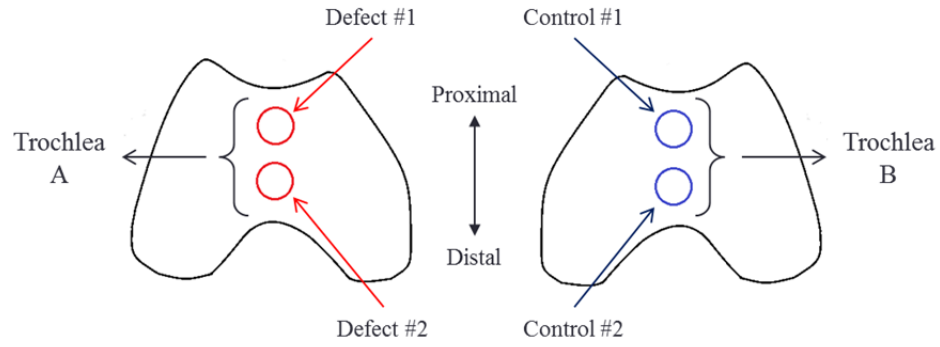

Figure 4: Animal testing model. Trochlea A contains two defects and trochlea B is left unoperated for control. Designation of trochlea A or B as the left or right joint in the horse was randomized. The two defects in trochlea A are filled with a repair group pair listed in Table 2. Designation of the treatments from each repair group pair into the proximal (defect #1) or distal (defect #2) defect was randomized. During sample harvesting, blocks of tissue containing one of the defects were removed from trochlea A. Similarly, blocks of tissue from the proximal (control #1) and distal (control #2) region were removed from trochlea B.

The defects in each operated joint were filled with one of the repair group pairs outlined in Table 2. In addition, the contralateral knee was left unoperated to be used as a control. The repair group pairs were chosen so that a defect filled with the MACI treatment was always used in conjunction with a defect filled with an ACI-Maix membrane or a defect left empty (see Table 2, repair group pair 1 and 2, respectively). This was to help determine if the efficacy of MACI grafts is influenced by the presence of another defect. In addition, one of the repair group pairs contained two empty defects (pair 3) to see how natural cartilage repair is affected in the presence of another defect.

One year after implantation, the horses were euthanized and the repair sites were harvested. The defects were then sectioned for a variety of tests. Osteochondral blocks 3 mm wide that extended 3 to 5 mm into the native cartilage were removed from the center of each defect for histologic examination. Two 3 mm biopsy punches were removed for compressive and shear testing. The remaining repair tissue was used for biochemical analysis. Samples of equal size were removed from the trochlea of the contralateral joint for control.

Histologic examination revealed higher chondrocyte population and type II collagen content in MACI grafts over ACI-Maix membrane and empty defects. Furthermore, MACI grafts improved defect fill and had a thicker proteoglycan-rich zone than the other repair groups. Biochemical analysis showed a higher GAG content but lower DNA content compared to the empty defects. Despite the promising results shown through histology and biochemical analysis, these traits are not necessarily indicative of good mechanical properties.

The procedures for compression and shear testing are shown below:

i. Confined Compression Testing

Full thickness samples of articular cartilage are harvested using a biopsy punch perpendicular to the articular surface. The cylindrical plug is placed in a confining chamber of matching cross sectional area (Figure 5). The side walls and bottom are rigid and impermeable. A porous loading platen is placed on top of the cartilage sample that allows water to freely pass through it. A testing apparatus places a compressive displacement on the tissue, causing the pressure within the cartilage plug to increase. After compression, water slowly escapes from the sample, reducing the internal pressure and allowing the tissue to relax. The displacement is maintained for an extended period of time as the tissue relaxes to an equilibrium pressure (σ_∞), and a load cell measures the pressure with time.

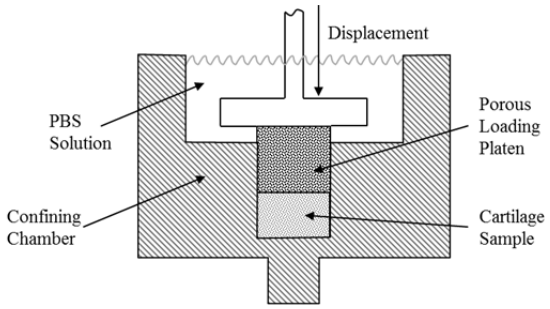

Figure 5: Cross sectional view of confined compression testing setup.

A typical stress-relaxation curve is shown in Figure 6A. This curve for stress σ and time t can be modeled using equations from poroelastic theory [16].

$$\sigma = -\left(\frac{H_A V_0}{h}\right)\left[t_0 - 2\sum_{n=1}^{\infty}\left(\frac{\tau}{n^2}e^{-n^2 t/\tau} - 1\right)\right] \quad (2)$$

where $\tau = \frac{h^2}{\pi^2 H_A k}$, dependent on the sample thickness h, permeability k, and aggregate modulus Ha. The summation in equation 2 can be simplified using only n=1 while still maintaining a high level of accuracy (see Appendix 1):

$$\sigma = -\left(\frac{H_A V_0}{h}\right)\left[t_0 - 2\left(\tau e^{-t/\tau} - 1\right)\right] \quad (3)$$

As the limit of $t \to \infty$, the stress equation is further simplified to a simple relationship between the strain and the aggregate modulus.

$$\sigma_\infty = H_A \varepsilon \quad (4)$$

The equilibrium stress for various strains are plotted to form a stress-strain curve (Figure 6B). Finally, the aggregate modulus is determined by the slope of the stress-strain curve at approximately 20-25% strain, and the hydraulic permeability is equal to:

$$k = \frac{h^2}{\pi^2 H_A \tau} \quad (5)$$

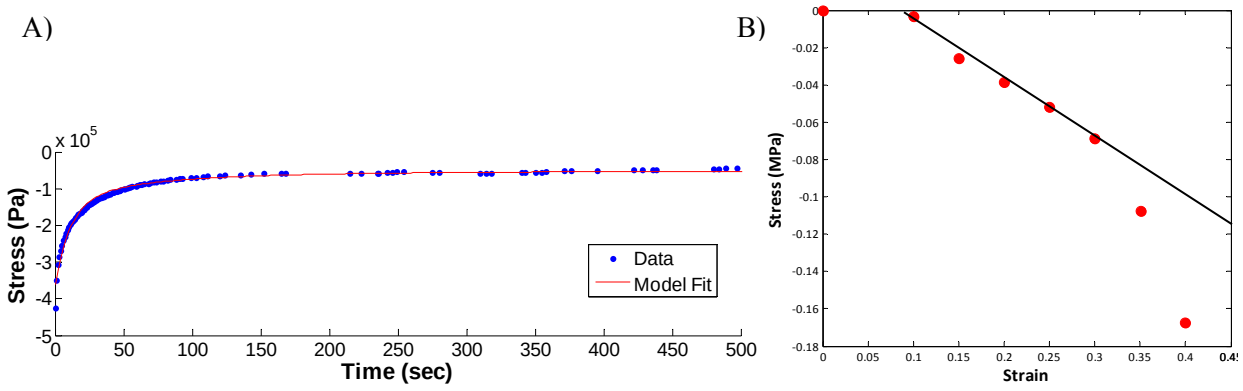

Figure 6: A) Stress-relaxation curve with poroelastic model fit; B) Resulting stress-strain curve derived from σ_∞ at varying levels of strain.

ii. Confocal Strain Mapping

Full thickness samples of articular cartilage are harvested using a biopsy punch perpendicular to the articular surface. The cylindrical plug is bisected longitudinally, exposing the transverse cross sectional area of the cartilage, from surface to deep zone tissue.

The sample is sheared using a tissue deformation imaging stage (TDIS), shown in Figure 7A. The sample is mounted to the TDIS by gluing the deep zone to a stationary plate (Figure 7B). Once mounted, the shearing plate is brought into contact with the articular surface. Previous research has shown that shear properties of cartilage are dependent on the amount of compressive strain on the sample [5]. Therefore, the amount of compression applied should be consistent between samples.

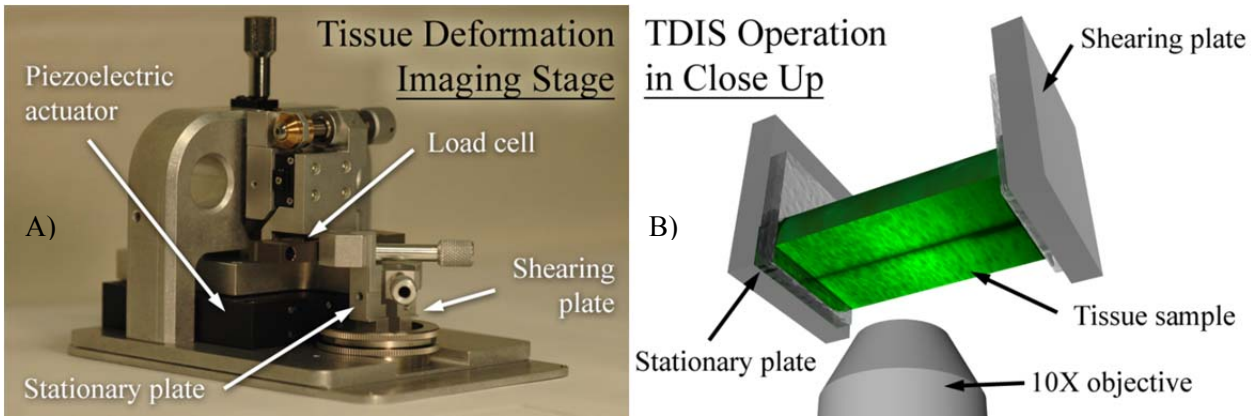

Figure 7: A) Picture of the TDIS, used to dynamically shear tissue samples; B) Cartilage is imaged from below using a 10X objective. A photobleached line is created that travels between the two plates.

The TDIS is mounted on an inverted confocal microscope and imaged using a 488 nm laser with a 10X objective lens. A line is photobleached perpendicular to the surface using the laser at full intensity (Figure 7B). The shearing plate moves parallel to the surface by a piezoelectric actuator, causing sinusoidal shear displacements in the sample. Previous research has shown that the shear properties of cartilage are also dependent on the frequency and amplitude of these sinusoidal displacements, and should therefore remain consistent between

samples [5]. As the sample is being sheared, the movements of the photobleached line are recorded and a load cell measures the force. The images are analyzed using custom MATLAB code that tracks the displacement of the line relative to its undeformed position.

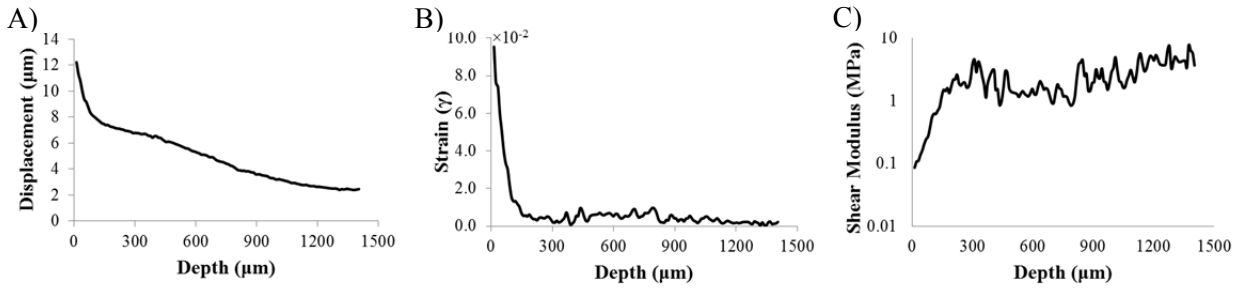

Figure 8: A) Maximum displacement of the tissue sample vs. depth from the articular surface; B) Strain vs. depth, determined from A); C) Shear modulus vs. depth, determined from B).

The MATLAB code tracks the displacement by locating the intensity minima of each image corresponding to the location of the line, and plots the maximum displacement $u_0(z)$ as a function of depth (Figure 8A). Simultaneously, the sinusoidal movements of the line are compared to the sinusoidal movements of the surface, giving the displacement phase angle $\delta_u(z)$. Because the shear stress τ_0 is uniform throughout the sample, the shear strain $\gamma_0(z)$ (Figure 8B) is given by:

$$\gamma_0(z) = \sqrt{\left[\frac{d}{dz}(u_0(z)\cos\delta_u)\right]^2 + \left[\frac{d}{dz}(u_0(z)\sin\delta_u)\right]^2} \quad (6)$$

When the phase angle is zero, the shear strain is simply the slope of the displacement vs. depth curve. Finally, the complex shear modulus $|G^*|(z)$ (Figure 8c) is given by:

$$|G^*|(z) = \frac{\tau_0}{\gamma_0(z)} \quad (7)$$

B. Summary of Research

1. Introduction

Articular cartilage has a limited ability for self-repair, allowing any defects left untreated to be susceptible to osteoarthritis [7]. Autologous chondrocyte implantation (ACI) has been shown to be an effective repair technique for full-thickness chondral defects [8] [30] [31]. The clinical application of ACI involves injecting cultured autologous chondrocytes into a defect and sealing the chondrocytes with either a periosteal or collagen flap sutured to the neighboring tissue [32]. In-vivo formation of hyaline-like cartilage has been observed using this repair technique [8]. However, complications stemming from leakage of cells into the joint, graft hypertrophy, delamination of the flap, and uneven distribution of chondrocytes within the defect have made ACI grafts a variable form of treatment [14].

A newer variation of ACI grafts is a process commonly known as matrix-induced autologous chondrocyte implantation (MACI ®, Genzyme Corporation). The clinical application of MACI involves seeding chondrocytes into a porcine-derived type I/type III collagen bilayer scaffold that is implanted into the chondral defect [9] [15]. The main benefit of this technique is its use of fewer surgical procedures, eliminating the need for sutures and a periosteal or collagen flap, and reducing the risk of cell leakage [9]. Furthermore, the collagen scaffolds help the chondrocytes maintain cell viability and phenotype [13].

There have been several studies that have shown the benefits of grafts using autologous chondrocytes, but few have analyzed the mechanical properties of the repaired tissue. Specifically, very few studies have looked at the compressive and shear properties of MACI grafts in a large animal model. Furthermore, there are no known studies that have looked at the local shear properties of these grafts, which have been shown to vary with depth in native tissue

[5] [33]. Characterizing the mechanical properties of MACI grafts is essential to understanding their proper functionality.

The purpose of this study was to characterize the mechanical properties of repaired articular cartilage using MACI grafts in an equine model. Two distinct types of mechanical testing were performed on repaired cartilage harvested from horses: 1) Confined compression testing to characterize the bulk compressive properties and measure the aggregate modulus (Ha) and hydraulic permeability (k); 2) Confocal strain mapping to measure the local shear modulus (G). These tests were performed on three repair groups: defects filled with MACI grafts, defects filled with the collagen membrane (ACI-Maix™, Matricel) alone, and defects left empty. All repair groups were compared to a contralateral control of native equine tissue.

2. Methods

2.1 Sample Preparation

A total of 27 skeletally mature horses (1.5-6 years of age, 300-400 kg weight) were approved and surgeries were performed according to the guidelines of the Institutional Animal Care and Use Committee (IACUC) at Cornell University. Two defects (15 mm diameter) were placed in a hind-limb of each horse. Specifically, one defect was placed in both the proximal and distal region of the trochlea in either the right or left joint, with the other joint left untouched for control. The two defects in each joint were filled with one of the following repair group pairs: 1) MACI grafts (group A) and ACI-Maix membranes (group B) (n=12); 2) Empty defects (group C) and MACI graft (group D) (n=12); 3) Empty defects in both sites (group E) (n=3). Location of defects in right or left joint, and treatment in proximal and distal regions was randomized. After

1 year, the horses were euthanized and samples were immediately harvested and snap-frozen using liquid nitrogen and stored at -80°C.

2.2 Confined Compression

Full thickness cylindrical plugs (3 mm diameter) were harvested from the defect region using a biopsy punch perpendicular to the articular surface. The plugs were thawed in a bath of PBS containing protease inhibitors. This procedure was repeated for samples harvested from the proximal and distal region of the trochlea in the control joint. Prior to testing, sample heights were measured using a caliper. Samples were placed in a 3 mm confining chamber, covered with a porous plug and PBS with protease inhibitors, and mounted to a Bose EnduraTEC ELF 3200 for testing. A series of 5% steps in compressive strain were imposed on each sample up to a total of 40% strain. For each step, the resultant load was measured for 10 minutes using a Honeywell 50lb load cell at a frequency of 1 Hz. The stress-relaxation curves were fit to a poroelastic model and analyzed using custom MATLAB code to calculate Ha and k [16] [34].

2.3 Confocal Strain Mapping

Full thickness cylindrical plugs (3 mm diameter) were harvested and thawed in the same manner as samples used for confined compression. The samples were bisected longitudinally into hemi-cylinders, exposed to 7 μg/mL 5-dichlorotriazinylaminofluorescein (5-DTAF) for 2 hours to uniformly stain the extracellular matrix, and rinsed in PBS for 30 minutes. Samples were tested as described before [5] [35]. Briefly, samples were glued to a tissue deformation imaging stage (TDIS) and compressed to 10% strain. The TDIS was mounted on an inverted Zeiss LSM 510 confocal microscope and imaged using a 488 nm laser. A line perpendicular to

the articular surface was photobleached using the laser at full intensity. Sinusoidal shear displacements were placed on the articular surface by the TDIS at a frequency of 0.1 Hz and amplitude of 16 μm, and the resultant forces were measured with a load cell. Simultaneously, images of the sample deforming were collected at 10 fps. Using custom MATLAB code, the intensity minima corresponding to the location of the photobleached line was tracked, and the local strains were determined from the slopes of that line. The local shear modulus (G) was calculated from the local strain and measured load.

2.4 Statistics

In order to determine if there was a significant difference ($p<0.05$ for all tests) between repaired and native cartilage, statistical analysis was performed between each repair group and native tissue. For the confined compression test, each defect could be matched to a contralateral control in the opposite joint. Comparison between repair groups and control was performed using a two-tailed paired t-test. For confocal strain mapping, it was not possible to harvest a defect sample from every joint. Therefore, a standard two-tailed t-test assuming unequal sample variance between groups was used to analyze the repair groups to control. For both mechanical tests, a one way analysis of variance (ANOVA) test was performed between all testing groups. Finally, each MACI group (A and D) and each empty group (C and E) were compared using a two-tailed t-test. All data groups are displayed as mean values with standard deviations noted by error bars.

3. Results

3.1 Confined Compression

Compression testing indicated that the average aggregate modulus for control articular cartilage ranged from 1.2-1.4 MPa, while the average hydraulic permeability ranged from 5-7 × 10^{-15} m^2/Pa-s. Both values are consistent with recorded values for native equine cartilage [18]. Chondral defects filled with MACI grafts had average aggregate modulus values that were 82% (group A) and 67% (group D) of the contralateral control, and were not statistically different (Figure 9A). The average hydraulic permeability values were 3 (group A) and 2.7 (group D) times higher than the control groups, but were still not statistically different (Figure 9B). Defects filled with ACI-Maix membranes (group B) had an average modulus value that was only 46% of the contralateral control, and those left empty were 63% (group C) and 51% (group E) of control. The average permeability values were 2.5 (group B), 2.3 (group C), and 6.3 (group E) times higher than control. All except one empty group were statistically different from control (group E), likely due to it having a much smaller sample size.

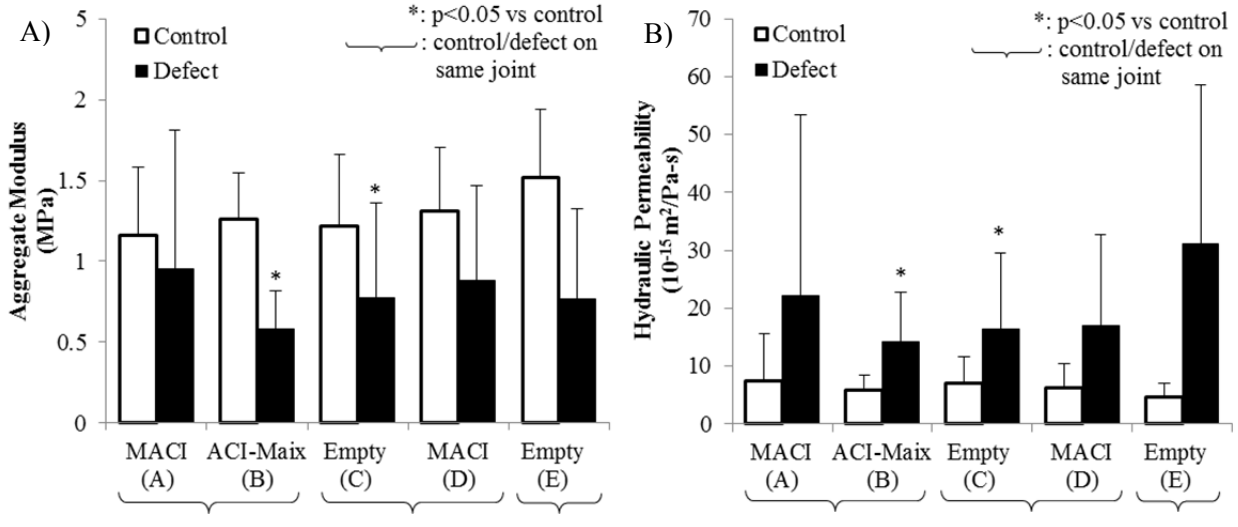

Figure 9: Average A) aggregate modulus and B) hydraulic permeability for each group and its contralateral control. All values expressed as mean ± standard deviation (n=12 for groups A-D, n=6 for group E).

3.2 Confocal Strain Mapping

The confocal strain mapping technique was used to find global and local shear modulus values. Shear testing indicated that the average global shear modulus for control cartilage ranged from 1.4-1.6 MPa, consistent with recorded values for native cartilage [33]. The average modulus for all repair groups was between 0.32 MPa and 0.68 MPa, significantly lower than the contralateral control groups (Figure 10). Specifically, chondral defects filled with MACI grafts had modulus values that were 48% (group A) and 20% (group D) of control. Defects filled with the ACI-Maix membrane (group B) and those left empty (groups C and E) had modulus values that were 22%, 38%, and 32% of control, respectively. Only one of the empty groups (group E) was not statistically different from control, again likely due to the smaller sample size.

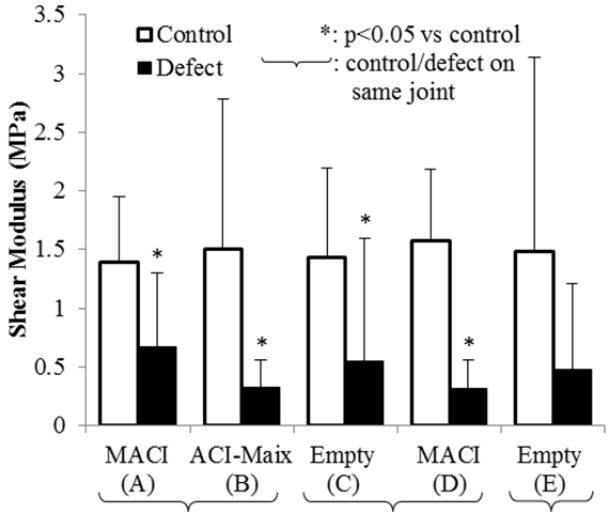

Figure 10: Global shear modulus for each repair group and its contralateral control. All values expressed as mean ± standard deviation (n=12 for control groups A-D, n=6 for control group E. n=8,5,7,7,3 for defect groups in order).

The local shear modulus (binned every 25 μm from the articular surface) of the control cartilage showed variation with depth, with the minimum modulus value occurring within 100 μm of the articular surface (Figure 11). In particular, the modulus dips near the surface and then increases to its maximum around 200 μm where it is relatively uniform throughout the deep

zone. The observed variation occurred on the same length scale regardless of the overall thickness of the sample. Such variations with depth are consistent with previously reported studies, though less prominent than variations shown in bovine and human tissue [35]. The tissue from defects displayed much less variation of the shear modulus with depth. Specifically, the MACI grafts and ACI-Maix membranes both displayed a slight dip in the local shear modulus from the surface to a local minimum within the first 100 μm, followed by a slight increase towards the deep zone. This is consistent with equine cartilage; however the value of the minimum and average shear stress was significantly lower than control. The empty defect showed minimal variation with depth, and was also significantly lower than control tissue.

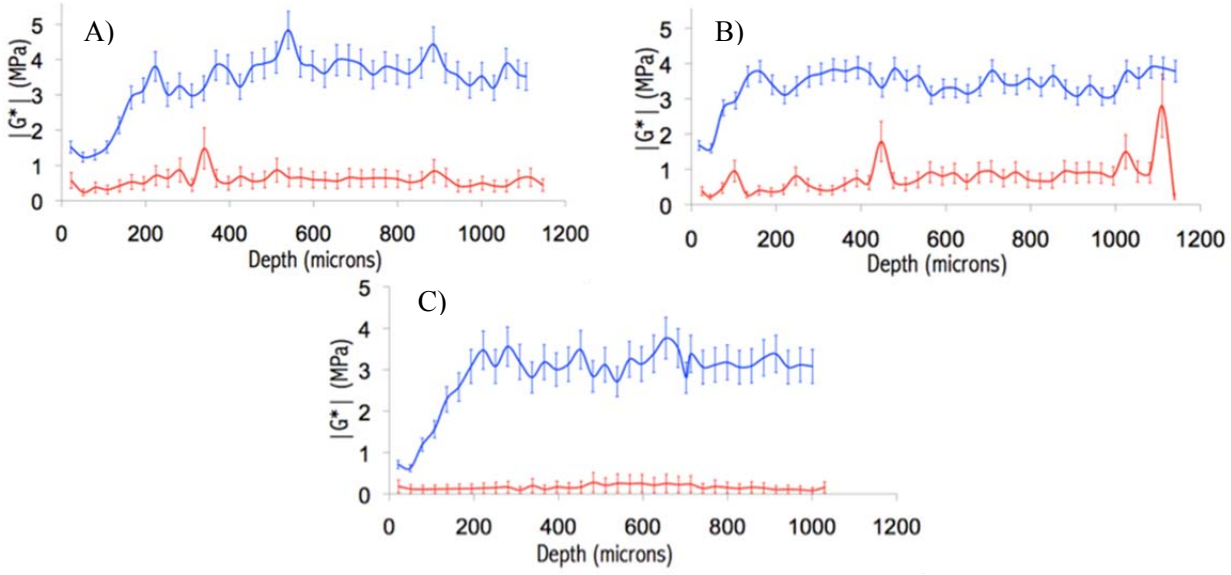

Figure 11: Local shear vs. depth from articular surface for A) MACI grafts, B) ACI-Maix membranes, C) empty defects. Control groups are shown in blue, defect groups are shown in red. All values are expressed as mean ± standard deviation (n=24,12,18 for all control groups A, B, and C, respectively. n=15,5,10 for defect groups A, B, and C, respectively).

3.3 Sample Thickness

The average sample thickness was consistent between all repair and control groups (Figure 12). Average repair group thickness ranged from 84-95% of control, with only one of the empty groups (group C) being statistically different from control in a paired t-test.

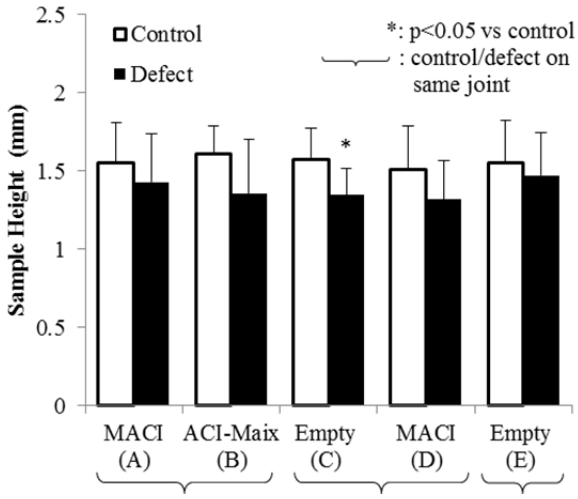

Figure 12: Average sample thickness for each repair group and its contralateral control. All values expressed as mean ± standard deviation (n=12 for groups A-D, n=6 for group E).

4. Discussion

The use of autologous chondrocytes to repair damaged cartilage has been increasingly pervasive due to its ability to develop hyaline-like cartilage within defects [8]. The addition of a collagen matrix to form MACI grafts has been shown to promote cell proliferation and reduce the risk of graft hypertrophy and cell leakage [14]. The results of this study demonstrate the mechanical properties of MACI repaired cartilage 1 year after repair.

There is limited previous research involving the mechanical performance of MACI grafts, which is arguably the most important parameter for successful defect repair [36]. Previous mechanical testing on cartilage that was repaired using autologous chondrocytes has yielded mixed results. Confined compression testing by Strauss *et al.* on ACI repaired equine tissue showed an aggregate modulus that was only 12% of native tissue (18). A MACI graft with a type II collagen membrane was shown by Lee *et al.* to have an aggregate modulus that was 15% of native tissue. Stiffness tests in an ovine model by Jones *et al.* and Russlies *et al.* showed that MACI grafts with a type I/type III collagen membrane ranged from 16-50% of native cartilage,

respectively [23] [24]. The MACI grafts in this study had an aggregate modulus that was 75% of native cartilage on average. Some of the increased performance of these MACI grafts may be attributed to the long term implant duration and the use of a large animal model.

Previous research on in situ static loading of human patellofemoral joints has shown mean and maximal compressive strains of 44% and 57%, respectively [37]. This indicates that the total compressive strain of 40% used in confined compression testing was physiologically relevant. Though previous research has been unclear as to the in vivo shear strains of articular cartilage, it has been shown in the data presented here and in previous studies that the region near the articular surface is more compliant than tissue in the deeper zone [5]. This shows that the relatively small shear strains applied on the surface during confocal strain mapping can cause larger local shear strains deeper in the tissue.

In confined compression testing, defects filled with MACI grafts performed similar to their contralateral control. The average aggregate modulus and hydraulic permeability of the MACI groups was not statistically different than the control tissue (Figure 9). During confocal strain mapping, defects performed significantly worse than their contralateral controls, regardless of the treatment option (Figure 10 and Figure 11). Furthermore, the MACI and ACI-Maix groups only showed slight variation in shear modulus with depth, and the empty groups showed little to no variation. The low shear modulus of the MACI grafts makes the repaired cartilage susceptible to future degradation. Furthermore, previous studies have shown that varying amounts of compression impact the shear modulus [33]. The cartilage was compressed to 10% strain in this study, but the performance of these grafts at other compressive strains is not yet known.

It can be noted that there is no distinguishable link shown in this study between compressive and shear properties. The promising results shown in compression were not shown

in shear testing. Furthermore, results from histologic assessment and biochemical analysis are not sufficient for predicting the mechanical properties. Histology and biochemistry done on MACI grafts found that they improve chondrocyte proliferation and GAG content over empty defects, but clearly these results weren't indicative of improvement in the shear properties. The relationship between structure and function is quite complex, and mechanical testing cannot be ignored when evaluating the performance of repaired cartilage.

C. Conclusion

Prior mechanical testing on autologous chondrocyte-based repair cartilage (outlined in Table 1) has typically focused on the compressive properties of the tissue and demonstrates that there are several variables that likely impact the efficacy of MACI treatments. The Genzyme study investigated the performance of MACI grafts that were implanted for one year in the trochlea of horses, and found a compressive modulus that was 75% of native tissue on average. This follows a general trend where experiments that utilized long implant durations in large animals, such as equine and human models, typically yielded better results. Because these grafts would ideally be used in human patients for as long a period as possible, the results of this study represent a more realistic analysis of the mechanical properties of MACI grafts.

Mean values for the measured mechanical properties had consistently large standard deviations for each testing group. A major source for this variation is the horses used for this study, whose backgrounds were from a variety of breeds and ages. In addition, measurement error could compound to yield slightly inaccurate results. For compressive tests, the aggregate modulus is dependent on the thickness measurement (equation 4). The hydraulic permeability is dependent on the squared value of the thickness measurement and the aggregate modulus (equation 5), and the high influence of the thickness measurement is likely responsible for the very large deviations shown in the permeability. Thickness measurements were taken with a digital caliper, making them highly susceptible to measurement error. For shear tests, the shear modulus is calculated using the sample cross sectional area (equation 7). If the sample is not completely flat on the articular surface, the area being sheared may not correspond to the measured area of the surface. Furthermore, the amount the sample is actually being compressed may not be consistent with other samples. Future improvements to this study would involve

minimizing the measurement error using more advanced measuring devices. The thickness of the sample could be measured by averaging a series of measurements found using a microscope. The regularity of the articular surface could be determined using a confocal microscope, and unlevel portions could be cut away from the sample. Minimizing the measurement error could reduce the variability in groups, and ultimately increase the statistical power of each testing group.

The Genzyme MACI grafts were able to restore the compressive properties of repaired cartilage to a level that is statistically similar to native cartilage. The grafts were unable to restore the shear properties to a normal level, which raises concerns as to the long term wear resistance of the tissue repair. A consideration for future repair techniques is attempting to replicate the local mechanical properties of native cartilage. Cartilage has a complex structure and composition, with the collagen fiber orientation and the chondrocyte and GAG concentrations varying with depth. This structure likely impacts the local compressive and shear modulus, which are more pliable near the surface and stiffer in the deep zone [(5) (38)]. The Genzyme study looked at the local shear properties of the repaired cartilage, but very little variation was noticed throughout the tissue. The compliant region near the surface may act as an energy dissipation mechanism and prevent wear [(5) (38)].

The success of repair tissue for chondral defects lies in the ability to replicate the structure and composition of articular cartilage. It is not sufficient to solely replicate the structure or the composition, as they both dictate the functional properties of the tissue. As discussed earlier, the majority of journal articles focus on histological examination and biochemical analysis. While clearly important in its own right, this information alone is not sufficient for assessing repair performance. Both the composition and the structure need to be fully understood for long-term evaluation and improvement of repair tissue [(22)].

Specifically looking at the results from the Genzyme study, it is very evident that histological and biochemical assessment alone cannot predict how repaired cartilage performs in a patient. In this study, MACI implants had higher collagen and GAG content, as well as higher chondrocyte population, over unfilled defects. However, these positive values were not indicative of the mechanical properties of the MACI grafts. The MACI compressive properties were indistinguishable from native tissue, but the shear properties were very poor regardless of repair group. If the argument is made that a higher collagen or GAG content leads to a better compressive modulus, clearly the same argument doesn't hold true for the shear modulus.

Statistical analyses through t-tests were able to determine differences between repair groups and their respective contralateral controls. However, the mechanical testing portion of this study was underpowered. One way ANOVA results indicate that there was not enough statistical power to detect differences between the repair groups. The experimental design was based on the histological and biochemical testing, but a larger sample size for each repair group would be needed to detect a difference in mechanical testing results.

For future studies, it would be interesting to determine if there were common histological and biochemical traits between samples that had strong mechanical performance. This could involve selecting a few of the best and a few of the worst performing samples from each testing group in terms of aggregate modulus, hydraulic permeability, and shear modulus. These samples could be compared to the histology and biochemical results from the experiments performed in the Nixon lab to see if there are any trends that can be found for both successful and unsuccessful grafts. Understanding why repaired cartilage has the mechanical properties it does remains a challenge to be addressed in order to further improve cartilage repair techniques.

Appendix

Appendix 1: Changes in aggregate modulus, time constant, and hydraulic permeability for higher order terms in the poroelastic model (shown for sample 877685).

	Ha (MPa)				τ (sec)				k (10^{-15} m^2/Pa-s)			
	n=1	n=2	n=3	n=4	n=1	n=2	n=3	n=4	n=1	n=2	n=3	n=4
877685	1.076	1.008	0.970	0.949	52.909	61.971	65.880	67.769	4.787	4.363	4.264	4.237
	0.298	0.286	0.280	0.276	9.575	11.081	11.773	12.156	71.602	64.469	61.975	60.896
	1.168	1.127	1.105	1.093	43.777	51.223	54.485	56.089	5.794	5.132	4.921	4.833
	0.277	0.257	0.246	0.241	16.147	18.717	19.847	20.431	31.543	29.329	28.896	28.652

Appendix 2: P-values and statistical powers from t-tests between repair groups and contralateral controls. Paired t-tests were performed on the aggregate modulus, hydraulic permeability, and thickness. Unpaired t-tests were performed on the shear modulus. All tests were standard parametric t-tests unless otherwise noted.

	Ha (MPa)		k (10^{-15} m^2/Pa-s)		G (MPa)		t (mm)	
Test	P	Power	P	Power	P	Power	P	Power
MACI (A)	0.442	0.050	0.301[w]	≤0.189	0.015	0.654	0.248	0.093
ACI-Maix (B)	<0.001	1.000	0.006	0.841	0.031[m]	≤0.350	0.057	0.391
Empty (C)	0.019	0.648	0.022	0.618	0.049	0.411	0.012	0.741
MACI (D)	0.069	0.349	0.052	0.415	<0.001[m]	≤0.999	0.064	0.363
Empty (E)	0.079	0.351	0.075	0.365	0.360	0.050	0.424	0.050

[w]: Wilcoxon Signed Rank Test
[m]: Mann-Whitney Rank Sum Test

Appendix 3: P-values and statistical powers from multiple comparison statistical tests. For aggregate modulus and hydraulic permeability, tests were performed for both normalized (each repair sample compared to contralateral control) and raw data. Comparisons between multiple testing groups were analyzed using a one way ANOVA. The two MACI groups were compared with a two-tailed t-test and combined to form one MACI and one empty testing group. Comparisons between the modified testing groups were performed using another one way ANOVA, with post-hoc results shown in appendix 4.

	Ha/Ha_{con}		Ha (MPa)		k/k_{con}		k (10^{-15} m^2/Pa-s)		G (MPa)	
Test	P	Power	P	Power	P	Power	P	Power	P	Power
One way ANOVA	0.728[k]	≤0.067	<0.001[k]	≤0.972	0.692[k]	≤0.327	0.002[k]	≤0.977	<0.001[k]	≤0.964
MACI t-test (A vs. D)	0.665[m]	≤0.050	0.885[m]	≤0.050	0.583[m]	≤0.050	0.795[m]	≤0.050	0.189[t]	0.137
Empty t-test (C vs. E)	0.543[m]	≤0.050	0.888[m]	≤0.050	0.281[m]	≤0.481	0.281[m]	≤0.194	0.667[m]	≤0.050
One way ANOVA[*]	0.492[k]	≤0.201	<0.001[k]	≤0.995	0.762[k]	≤0.049	<0.001[k]	≤0.976	<0.001[k]	≤0.992

[*]: Modified one way ANOVA with four testing groups: MACI, ACI-Maix, Empty, and Control
[k]: Kruskal-Wallis ANOVA on Ranks
[m]: Mann-Whitney Rank Sum Test
[t]: Standard t-test

Appendix 4: Post-hoc results for modified one way ANOVA test (Dunn's method).

	Ha (MPa)	k (10^{-15} m^2/Pa-s)	G (MPa)
Test	P<0.05	P<0.05	P<0.05
MACI vs. Con	Yes	No	Yes
ACI-Maix vs. Con	Yes	Yes	Yes
Empty vs. Con	Yes	Yes	Yes
MACI vs. ACI-Maix	No	No	No
MACI vs. Empty	No	No	No
ACI-Maix vs. Empty	No	No	No

Appendix 5: Mechanical testing data for confined compression testing and confocal strain mapping.

MACI grafts (Group A)

Sample	Defect			Control		
	Ha (MPa)	k (10^{-15} m^2/Pa-s)	G (MPa)	Ha (MPa)	k (10^{-15} m^2/Pa-s)	G (MPa)
877594	0.749	5.967	0.968	1.128	6.037	0.976
877596	2.272	1.765	0.050	0.874	8.968	0.516
877597	2.881	0.814	1.021	1.792	2.460	0.768
877668	0.493	21.001	N/A	1.793	4.346	0.949
877681	0.813	6.420	N/A	0.297	31.585	0.523
877683	0.474	24.987	N/A	0.852	4.994	1.086
877685	0.298	71.602	0.029	1.076	4.787	0.918
877693	1.259	1.354	0.554	0.941	4.160	0.866
877695	1.191	4.629	0.088	1.214	7.079	1.498
877697	0.287	94.305	N/A	1.100	3.802	0.203
877699	0.334	24.391	0.626	0.955	9.411	1.093
877701	0.384	9.527	0.354	1.904	1.415	0.510

ACI-Maix membranes (Group B)

Sample	Defect			Control		
	Ha (MPa)	k (10^{-15} m^2/Pa-s)	G (MPa)	Ha (MPa)	k (10^{-15} m^2/Pa-s)	G (MPa)
877594	0.728	4.452	N/A	1.006	4.875	0.428
877596	0.778	10.446	N/A	1.176	7.584	0.487
877597	0.712	8.174	0.481	1.501	2.238	0.095
877668	0.45	16.623	0.222	0.825	11.277	0.121
877681	0.983	15.563	N/A	1.472	6.67	1.54
877683	0.572	13.36	N/A	1.052	8.862	0.96
877685	0.277	31.543	0.149	1.168	5.794	0.798
877693	0.487	17.108	0.066	1.342	2.959	1.42
877695	0.263	18.308	N/A	1.323	7.725	0.713
877697	0.543	2.848	N/A	1.303	4.593	0.798
877699	0.324	26.099	0.04	1.906	3.021	0.642
877701	0.867	5.988	N/A	1.05	3.781	N/A

Empty (Group C)

Sample	Defect			Control		
	Ha (MPa)	k (10^{-15} m^2/Pa-s)	G (MPa)	Ha (MPa)	k (10^{-15} m^2/Pa-s)	G (MPa)
877595	1.123	9.420	0.202	1.850	2.761	0.027
877679	2.246	1.439	0.076	1.535	3.241	0.818
877680	0.908	8.798	N/A	1.639	3.548	1.235
877684	0.295	19.960	1.412	0.977	17.454	0.674
877686	0.551	28.679	0.085	0.916	8.682	0.866
877691	1.408	2.467	N/A	1.007	4.896	0.526
877692	0.412	25.452	N/A	0.990	4.629	0.905
877694	0.464	7.013	N/A	1.056	7.364	1.057
877696	0.593	16.519	N/A	2.089	2.630	0.765
877698	0.747	5.414	0.030	0.983	8.971	0.257
877702	0.187	43.650	0.092	0.787	6.886	0.844
877745	0.336	29.208	0.327	0.807	13.502	0.930

MACI grafts (Group D)

Sample	Defect			Control		
	Ha (MPa)	k (10^{-15} m^2/Pa-s)	G (MPa)	Ha (MPa)	k (10^{-15} m^2/Pa-s)	G (MPa)
877595	1.182	4.156	N/A	1.505	3.282	0.974
877679	0.410	11.842	0.020	1.555	3.544	0.807
877680	1.699	1.744	0.524	1.723	4.054	0.772
877684	1.001	5.903	0.053	1.233	10.635	1.069
877686	0.250	43.570	0.450	0.904	5.985	0.923
877691	0.281	38.508	0.191	1.408	4.499	1.304
877692	0.792	13.465	0.217	1.551	3.503	1.007
877694	0.963	11.207	N/A	1.050	9.197	0.358
877696	0.244	41.554	N/A	0.865	5.023	0.984
877698	0.401	22.559	N/A	1.920	3.039	1.170
877702	1.442	1.863	N/A	1.469	4.000	0.755
877745	1.923	7.094	0.152	0.578	17.608	1.394

Empty (Group E)

Sample	Defect			Control		
	Ha (MPa)	k (10^{-15} m^2/Pa-s)	G (MPa)	Ha (MPa)	k (10^{-15} m^2/Pa-s)	G (MPa)
877678	0.306	71.872	N/A	2.044	2.647	0.276
877678	0.870	12.912	N/A	1.294	7.790	0.075
877687	1.672	2.337	0.068	1.415	3.887	0.280
877687	0.257	51.998	0.510	1.166	4.110	1.571
877690	0.388	38.035	0.028	2.048	2.370	1.271
877690	1.112	10.053	N/A	1.137	7.431	1.129

References

1. Nap, R.J., and Szleifer, I. "Structure and Interactions of Aggrecans: Statistical Thermodynamic Approach." *Biophysical Journal* 95.10 (2008): 4570-583.

2. Martin, B., Burr, D., and Sharkey, N. *Skeletal Tissue Mechanics*. New York: Springer, 1998.

3. Buckwalter, J.A., Mow, V.C., and Ratcliffe, A. "Restoration of Injured or Degenerated Articular Cartilage." *Journal of the American Academy of Othopaedic Surgeons* 2(4) (1994): 192-201.

4. Mow, V.C., and Hayes, W. *Basic Orthopaedic Biomechanics*. Philadelphia: Lippincott-Raven, 1997.

5. Buckley, M.R., Gleghorn J.P., Bonassar, L.J., Cohen, I. "Mapping the Depth Dependence of Shear Properties in Articular Cartilage." *Journal of Biomechanics* 41.11 (2008): 2430-437.

6. Inerot, S., Heinegard, D., Audell, L., and Olsson, S. "Articular-Cartilage Proteoglycans in Aging and Osteoarthritis." *Biochemical Journal* 169 (1978): 143-56.

7. Mankin, H. "The Response of Articular Cartilage to Mechanical Injury." *The Journal of Bone and Joint Surgery* 64 (1982): 460-66.

8. Brittberg, M., Lindahl, A., Nilsson, A., Ohlsson, C., Isaksson, O., and Peterson, L. "Treatment of Deep Cartilage Defects in the Knee with Autologous Chondrocyte Transplantation." *New England Journal of Medicine* 331.14 (1994): 889-95.

9. Cherubino, P., Grassi, Bulgheroni, and Ronda. "Autologous Chondrocyte Implantation Using a Bilayer Collagen Membrane: A Preliminary Report." *Journal of Orthopaedic Surgery* 11(1) (2003): 10-15.

10. Brittberg, M. "Cell Carriers as the Next Generation of Cell Therapy for Cartilage Repair: A Review of the Matrix-Induced Autologous Chondrocyte Implantation Procedure." *The American Journal of Sports Medicine* 38.6 (2010): 1259-271.

11. Jacobi, M., Villa, V., Magnussen, R.A., and Neyret, P. "MACI - a New Era?" *Sports Medicine, Arthroscopy, Rehabilitation, Therapy & Technology* 3:10 (2011)

12. Frankel, S., Toolan, B., Menche, D., Pitman, M., and Pachence, J. "Chondrocyte Transplantation Using a Collagen Bilayer Matrix for Cartilage Repair." *The Journal of Bone and Joint Surgery* 79-B.No. 5 (1997).

13. Gigante, A., Bevilacqua, C., Cappella, M., Manzotti, S., and Greco, F. "D Articular Cartilage: Influence of the Scaffold on Cell Phenotype and Proliferation." *Journal of Material ScienceL Materials in Medicine* 14.8 (2003): 713-16.

14. Sohn, D.H., Lottman, L.M., Lum, L.Y., Kim, S.G., Pedowitz, R.A., Coutts, R.D., and Sah, R.L. "Effect of Gravity on Localization of Chondrocytes Implanted in Cartilage Defects." *Clinical Orthopaedics and Related Research* 394 (2002): 254-62.

15. Willers, C., Chen, J.,Wood, D., Xu, J., and Zheng, M.H. "Autologous Chondrocyte Implantation with Collagen Bioscaffold for the Treatment of Osteochondral Defects in Rabbits." *Tissue Engineering* 11.7-8 (2005): 1065-076.

16. Mow, V.C., Kuei, S.C., Lai, W.M., and Armstrong, C.G. "Biphasic Creep and Stress Relaxation of Articular Cartilage in Compression: Theory and Experiments." *Journal of Biomechanical Engineering* 102.1 (1980): 73.

17. Gratz, K.R., Wong, V.W., Chen, A.C., Fortier, L.A., Nixon, A.J., and Sah, R.L. "Biomechanical Assessment of Tissue Retrieved after in Vivo Cartilage Defect Repair: Tensile Modulus of Repair Tissue and Integration with Host Cartilage."*Journal of Biomechanics* 39.1 (2006): 138-46.

18. Strauss, E.J., Goodrich, L.R., Chen, C., Hidaka, C., and Nixon, A.J. "Biochemical and Biomechanical Properties of Lesion and Adjacent Articular Cartilage After Chondral Defect Repair in an Equine Model." *American Journal of Sports Medicine* 33.11 (2005): 1647-653.

19. Chiang, H., Kuo, T-F., Tsai, C-C., Lin, M-C., She, B-R., Huang, Y-Y., Lee, H-S., Shieh, C-S., Chen, M-H., Ramshaw, J.A.M., Werkmeister, J.A., Tuan, R.S., and Jiang, C-C. "Repair of Porcine Articular Cartilage Defect with Autologous Chondrocyte Transplantation." *Journal of Orthopaedic Research* 23.3 (2005): 584-93.

20. Laasanen, M.S., Töyräs, J., Vasara, A.I., Hyttinen, M.M., Saarakkala, S., Hirvonen, J., Jurvelin, J.S., and Kiviranta, I. "Mechano-Acoustic Diagnosis of Cartilage Degeneration and Repair." *The Journal of Bone and Joint Surgery* 85-A.2 (2003): 78-84.

21. Peterson, L., Brittberg, M., Kiviranta, I., Akerlund, E.L., and Lindahl, A. "Autologous Chondrocyte Transplantation: Biomechanics and Long-Term Durability." *The American Journal of Sports Medicine* 30.1 (2002): 2-12.

22. Henderson, I., Lavigne, P., Valenzuela, H., and Oakes, B. "Autologous Chondrocyte Implantation: Superior Biologic Properties of Hyaline Cartilage Repairs."*Clinical Orthopaedics and Related Research* 455 (2007): 253-61.

23. Russlies, M., Rüther, P., Köller, W., Stomberg, P., and Behrens, P. "Biomechanical Properties of Cartilage Repair Tissue after Different Cartilage Repair Procedures in Sheep." *Zeitschrift Für Orthopädie* 141.4 (2003): 465-71.

24. Jones, C.W., Willers, C., Keogh, A., Smolinski, D., Fick, D., Yates, P.J., Kirk, T.B., and Zheng, M.H. "Matrix-induced Autologous Chondrocyte Implantation in Sheep: Objective Assessments including Confocal Arthroscopy." *Journal of Orthopaedic Research* 26.3 (2008): 292-303.

25. Lee, C.R., Grodzinsky, A.J., Hsu, H-P., Martin, S.D., and M. Spector. "Effects of Harvest and Selected Cartilage Repair Procedures on the Physical and Biochemical Properties of Articular Cartilage in the Canine Knee." *Journal of Orthopaedic Research* 18.5 (2000): 790-99.

26. Lee, C.R., Grodzinsky, A.J., Hsu, H-P., and Spector, M. "Effects of a Cultured Autologous Chondrocyte-seeded Type II Collagen Scaffold on the Healing of a Chondral Defect in a Canine Model." *Journal of Orthopaedic Research* 21.2 (2003): 272-81.

27. Filová, E., Jelínek, F., Handl, M., Lytvynets, A., Rampichová, M., Varga, F., Cinátl, J., Soukup, T., Trc, T., and Amler, E. "Novel Composite Hyaluronan/Type I Collagen/Fibrin Scaffold Enhances Repair of Osteochondral Defect in Rabbit Knee." *Journal of Biomedical Materials Research Part B: Applied Biomaterials* 87.2 (2008): 415-24.

28. Peretti, G.M., Randolph, M.A., Zaporojan, V., Bonassar, L.J., Xu, J-W., Fellers, J.C., and Yaremchuk, M.J. "A Biomechanical Analysis of an Engineered Cell-Scaffold Implant for Cartilage Repair." *Annals of Plastic Surgery* 46.5 (2001): 533-37.

29. Liu, Y., Chen, F., Liu, W., Cui, L., Shang, Q., Xia, W., Wang, J., Cui, Y., Yang, G., Liu, D., Wu, J., Xu, R., Buonocore, S., and Cao, Y. "Repairing Large Porcine Full-Thickness Defects of Articular Cartilage Using Autologous Chondrocyte-Engineered Cartilage." *Tissue Engineering* 8.4 (2002): 709-21.

30. Petersen, W., Zelle, S.Z., and Zantop, T. "Arthroscopic Implantation of a Three Dimensional Scaffold for Autologous Chondrocyte Transplantation." *Archives of Orthopaedic and Trauma Surgery* 128.5 (2008): 505-08.

31. Ruano-Ravina, A., and Jato Diaz, M. "Autologous Chondrocyte Implantation: A Systematic Review." *Osteoarthritis and Cartilage* 14.1 (2006): 47-51.

32. Bartlett, W., Skinner, J.A., Gooding, C.R., Carrington, R.W.J., Flanagan, A.M., Briggs, T.W.R., and Bentley, G. "Autologous Chondrocyte Implantation versus Matrix-induced Autologous Chondrocyte Implantation for Osteochondral Defects of the Knee: A Prospective, Randomized Study." *Journal of Bone and Joint Surgery - British Volume* 87-B.5 (2005): 640-45.

33. Wong, B.L., Bae, W.C., Chun, J., Gratz, K.R., Lotz, M., and Sah, R.L. "Biomechanics of Cartilage Articulation: Effects of Lubrication and Degeneration on Shear Deformation." *Arthritis & Rheumatism* 58.7 (2008): 2065-074.

34. Chang, S.C.N., Rowley, J.A., Tobias, G., Genes, N.G., Roy, A.K., Mooney, D.J., Vacanti, C.A., and Bonassar, L.B. "Injection Molding of Chondrocyte/alginate Constructs in the Shape of Facial Implants." *Journal of Biomedical Materials Research* 55.4 (2001): 503-11.

35. Buckley, M.R., Bergou, A.J., Fouchard, J., Bonassar, L.J., and Cohen, I. "High-resolution Spatial Mapping of Shear Properties in Cartilage." *Journal of Biomechanics* 43.4 (2010): 796-800.

36. Poole, R. "What Type of Cartilage Repair Are We Attempting to Attain?" *The Journal of Bone and Joint Surgery* 85-A.2 (2003): 40-44.

37. Herberhold, C., Faber, S., Stammberger, T., Steinlechner, M., Putz, R., Englmeier, K.H., Reiser, M., and Eckstein, F. "In Situ Measurement of Articular Cartilage Deformation in Intact Femoropatellar Joints under Static Loading." *Journal of Biomechanics* 32.12 (1999): 1287-295.

38. Schinagl, R.M., Ting, M.K., Price, J.H., and Sah, R.L. "Video Microscopy to Quantitate the Inhomogeneous Equilibrium Strain within Articular Cartilage during Confined Compression." *Annals of Biomedical Engineering* 24.4 (1996): 500-12.